PS/RF/Note 98-09
CLIC-Note 358
April 17, 1998

Modeling a 30 GHz Waveguide Loaded Detuned Structure for the Compact Linear Collider (CLIC)

Micha Dehler

Introduction

Previous research on damped as well as detuned structures for CLIC has led to the following general conclusions.

Damped structures can in principle achieve the required wakefield performance for the CLIC multi bunch option, if ideally matched broad band loads are assumed. In order to get a broad band damping of the dipole spectrum over several bands, a T-shaped waveguide cross section has to be used. The ability to make a sufficiently good broad-band load, and the fabrication difficulties associated with the reduced rigidity of the discs are both however major concerns.

Detuning, on the other hand, has the advantage of affecting all dipole bands and of being able to create a fast roll-off of the transverse wake with much reduced mechanical difficulties. The critical point of a purely detuned design is recoherence leading to high long range wake levels.

The complementarity of these two methods has lead to the development of hybrid structures, employing both methods, as in the SLAC damped detuned structure DDS. The SLAC DDS uses a fully-fledged Gaussian detuning to obtain an optimum roll off behavior, combined with a slight damping to suppress recoherence effects. For the first few bunches, the wake function is largely determined by detuning, it is only in the long range, that the damping becomes effective. The drawback in this case is the high precision required: Due to the fact, that all cells are coupled to one set of manifolds, the cell to manifold coupling influences also the cell to cell coupling. Similar to weak damping, an exaggerated damping also leads to ripples in the transverse impedance and a deteriorated performance. The optimum amount of damping is therefore closely related to the detuning, so that certain mechanical imprecisions are felt twice, giving a non ideal detuning and over/undercoupling to the manifold.

For a CLIC multi bunch structure, the following requirements would therefore be

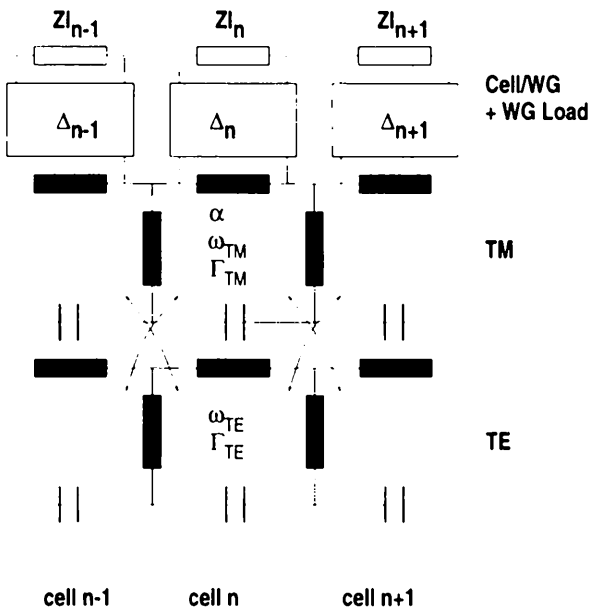

Figure 1: Equivalent circuit diagram for a waveguide damped detuned structure.

desirable. The structure should not rely on a high degree of optimization for the detuning nor for the damping employed. Specifically, a more primitive constant gradient like detuning is to be preferred. The damping mechanism should use radial waveguide with a simple rectangular cross section, not having the restrictions of the SLAC DDS on the amount of damping. The requirements for the waveguide load should be limited, allowing for high reflection coefficients and limited bandwidths.

For this type of design, a model is required, which takes into account the collective behavior of the detuned cells as well as the coupling mechanism between the waveguide load and the cavity. A relatively good description of the cell to cell coupling is given by the equivalent circuit model used by SLAC, describing the lower two dipole pass bands via two connected chains of resonators. To this a coupling network has to be added. Since the wakes (given by voltages in the equivalent circuit) are directly calculated from the solution of the inhomogeneous equation system, the reflection coefficient of the load can be incorporated into the circuit directly in the form of a table of scattering parameters calculated by MAFIA.

General Description

A standard double band circuit is chosen for the model. The damping waveguide, coupling only to the TM part of the circuit, is modeled by a resistor in parallel with the TM inductance (figure 1). The determination of the cell parameters follows the procedure of Bane and Gluckstern [1], where only the frequencies of the 0- and π-modes are used. The calculation of the TE type resonances is straight forward, there

is no coupling to the waveguides and the frequencies can be obtained directly from the MAFIA calculation giving the circuit parameters as:

$$x = \frac{1}{\omega_{TE}^2} = \frac{1}{2}\left(\frac{1}{\omega_{0,TE}^2} + \frac{1}{\omega_{\pi,TE}^2}\right)$$

$$k = \Gamma x = \frac{1}{2}\left(\frac{1}{\omega_{0,TE}^2} - \frac{1}{\omega_{\pi,TE}^2}\right)$$

For the 0 and π phase advances, the TM part of the circuit consists of a standard LC circuit with/without coupling inductances in parallel with the waveguide impedance. The procedure is inspired by that of Kroll [2], employing multiple frequency domain calculations in combination with short circuited waveguides of variable length in order to determine cell resonance, cell to cell coupling and cell to waveguide coupling. With the resonance frequencies for the 0 and π phase advances, the cell resonance and cell to cell coupling can be calculated.

Fitting Procedure

For the TM resonance with zero phase advance, the resulting circuit consists of a LC circuit in parallel with the waveguide conductance, which is given by:

$$Y = -\frac{A\beta}{j\omega}\cot\beta l$$

The impedance of the LC circuit, normalized to the waveguide impedance $\frac{\omega}{A\beta}$, is

$$Z = \frac{j\beta AL}{1-\omega^2/\omega_0^2} = \frac{j\beta\alpha}{1-\omega^2/\omega_0^2}$$

with $\alpha = AL$ and $\omega_0^2 = \frac{1}{LC}$.

The corresponding reflection coefficient seen by the waveguide is

$$r = \frac{\omega^2 + j\beta\alpha\omega_0^2 - \omega_0^2}{\omega^2 - j\beta\alpha\omega_0^2 - \omega_0^2}$$

having a absolute value of one and a complex phase of:

$$\phi_r = 2\tan^{-1}\frac{j\beta\alpha\omega_0^2}{\omega^2 - \omega_0^2}$$

The phase of the reflection coefficient of the shorted waveguide is determined by the length and is given by:

$$\phi_w = 2\beta(l + \Delta)$$

For the resonance condition to hold true, both phases have to be equal, this leads to:

$$\beta(\omega)(l+\Delta) = \tan^{-1}\frac{j\beta(\omega)\alpha\omega_0^2}{\omega^2-\omega_0^2}$$

The unknowns are the resonant frequency ω_0, the coupling coefficient α and Δ as a correction term for the length. The transition from cavity to waveguide introduces additional phase shifts, which are described in [2] by a constant complex phase in the frequency domain, which would give a complex, non causal, time domain function. Here the phase shift is incorporated in the form of an electrical length of the waveguide, which is different from the mechanical one, which is described by the additional length Δ. One additional remark should be made, when defining the waveguide length. Instead of measuring the waveguide length from the cavity wall, and in order to facilitate the mechanical construction, the length is defined to start at a distance of 4 mm from the cavity axis.

In order to get a fast solution, the following approach is used. First the three point formula from Kroll is used to determine an equivalent circuit assuming a constant waveguide impedance. From this, first estimates of the parameters are obtained via

$$\alpha = \frac{2v}{\omega_0\beta(\omega_0)}$$

and

$$\Delta = \frac{\chi}{\beta(\omega_0)}$$

These are taken as starting values for a nonlinear fitting procedure. Because of the ambiguity of the tan function, the modified equation

$$\sin\left(\beta(\omega)(l+\Delta) - \tan^{-1}\frac{\beta(\omega)\alpha\omega_0^2}{\omega^2-\omega_0^2}\right) = 0$$

is used for the solver. This gives the TM_0 resonance frequency as well as first estimates for the coupling coefficient α and the length Δ.

The TM_π resonance as well as final values for α and Δ are obtained by a second nonlinear fit using the eigenvalue equation:

$$\sin\left(\beta(\omega)(l+\Delta) - \tan^{-1}\left(-\beta(\omega)\alpha\left(1+\frac{\omega^2\frac{\omega_\pi^2}{\omega_0^2}}{\omega_\pi^2-\omega^2}\right)\right)\right) = 0$$

The 0-mode frequency ω_0 is given by the previous set of calculations, the values for frequencies and waveguide lengths come from calculations with a phase advance of π.

A set of results is shown in table 1. α and Δ, the parameters describing the cavity/waveguide coupling are obtained twice, once from the fit for the TM_π modes and once for the TM_0 modes. Comparing these two sets is an additional check for the quality of the approximation. Since the lower dipole band is the dominant contributor

cell	I	II	III
a/mm	1.8	2.0	2.2
b/mm	3.87	3.96	4.09
TE_0/GHz	37.43	34.83	31.97
TE_π/GHz	52.34	52.12	51.50
TM_0/GHz	42.56	41.84	40.85
TM_π/GHz	38.88	37.90	36.96
$\alpha \cdot 10^4$	1.42	1.43	1.41
Δ/mm	0.70	0.59	0.35
$\tilde{\alpha} \cdot 10^4$	1.36	1.32	1.30
$\tilde{\Delta}$/mm	0.64	0.60	0.34

Table 1: Equivalent circuit parameters for three different generic cells. $\tilde{\alpha}$ and $\tilde{\Delta}$ denote the values obtained by the TM_0 fit. For the precise definition of Δ see page 4.

to the wake, the values stemming from the TM_π fit are used in the circuit. With this, the TM circuit resonance and cell to cell coupling is given as:

$$\hat{x} = \frac{1}{\omega_{TM}^2} = \frac{1}{2}\left(\frac{1}{\omega_{0,TM}^2} + \frac{1}{\omega_{\pi,TM}^2}\right)$$

$$\hat{k} = \Gamma\hat{x} = \frac{1}{2}\left(\frac{1}{\omega_{\pi,TM}^2} - \frac{1}{\omega_{0,TM}^2}\right)$$

Dispersion and Impedances

The dispersion relation is very similar to the standard two band formula. The cell resonance (denoted by Bane/Gluckstern with $\hat{x} = 1/\omega_{TM}^2$) simply has to be modified by a factor describing the waveguide coupling and the reflection of the load S_{11} giving

$$\hat{x} = \frac{1}{\omega_{TM}^2}\,\frac{1 + j\alpha\beta\Gamma + S_{11}(1 - j\alpha\beta\Gamma)}{1 + j\alpha\beta + S_{11}(1 - j\alpha\beta)}$$

with $\Gamma = \hat{k}/\hat{x}$ the normalized cell to cell coupling.

Using this equation, the Brillouin diagram for a cavity with shorted wave guides can be calculated. The result of such an approach is shown in figure 2, together with the corresponding MAFIA results. It can be seen, that a relatively good agreement for frequencies up to 55 GHz can be obtained. For the given waveguide geometry, higher order waveguide modes start to propagate above this frequency, influencing the dispersion curves.

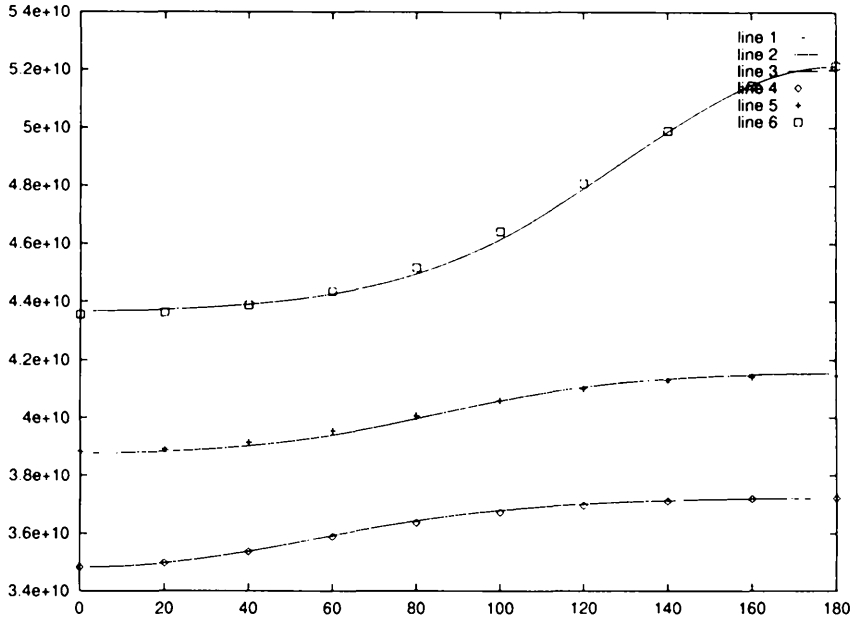

Figure 2: Dispersion diagram for cell II with 6 mm waveguide attached. Solid lines are results from the equivalent circuit model, the markers are MAFIA results.

The topological structure of the circuit equations corresponds to that of a purely detuned structure. The difference lies only in the resonance frequency of the TM circuit, as has been said before.

With the unknown proportionality factor A, the synchronous impedance seen by the beam becomes with $\lambda = 1/\omega^2$ and ϕ as the synchronous phase advance:

$$Z(\omega) = \frac{A}{j\omega}\left(1 + \frac{\lambda(\hat{x} - \lambda + \hat{k}\cos\phi)}{(x-\lambda)(\hat{x}-\lambda) + \cos\phi(\hat{k}(x-\lambda) - k(\hat{x}-\lambda)) - k\hat{k}}\right)$$

Kick factors

The only thing missing for a complete determination of the impedance function is the factor A, the equivalent of the single bunch loss factor. The extraction of a single mode kick factor by a time domain calculation is not easily possible with good accuracy, since a large number of cells would have to be calculated in order to see the synchronous kick in the wake potential. Additionally the peaks in the corresponding impedance function are spread out, so that neighboring resonances overlap.

Here, an alternative method is used, which consists of calculating the synchronous loss factors of a cavity with ideally shorted waveguides and comparing these with the residuals of the corresponding equivalent circuit impedance. If the equivalent circuit were a perfect description of the cavity, it would suffice to compare only for one resonant frequency. In order to improve the calculation, the sum of the residuals in the lower frequency region is used to derive the kick factor.

	Equivalent circuit			MAFIA	
ϕ_s	f/GHz	raw residual	scaled residual	f/GHz	k_{loss} (V/pC/m/mm^2)
142.8	35.71	0.475	71.29	35.72	76.31
153.2	38.30	2.152	323.1	38.29	325.0
177.0	44.25	0.285	42.11	44.11	41.60
204.5	51.11	0.040	5.990	51.11	0.160

Table 2: Intermediate results for the calculation of the dipole loss factor. The scaling factor is given by the ratio of the sum of the MAFIA loss factors and the sum of the raw residuals.

The set of results for cell II is shown in table 2. The raw residuals are extracted numerically from the impedance function by first determining the zeros of the admittance $Y = 1/Z$. The raw residual is given by:

$$\frac{1}{k_{raw}} = \frac{\partial Y}{\partial \omega}$$

Dividing the sum of the loss factors calculated by MAFIA by the sum of the raw residuals gives the scaling factor. The transverse kick in V/(pC m mm) is derived from:

$$w_t(\omega) = 1000\frac{c_0}{\omega} A \cdot Z(\omega)$$

It is interesting to note in table 2, that the distribution of the loss factors calculated by MAFIA corresponds quite well to that of the equivalent circuit. One typical exception is the resonance at 51 GHz, where the equivalent circuit loss factor is larger than the original one. This effect is due to the double band model describing the loss/kick factor via the partitioning of the modal energy between the TE and TM circuits and is similar to the effect seen in a purely detuned analysis. None-the-less the fact, that the equivalent circuit overstates the contribution of the second dipole band, gives an additional security margin to the design and therefore is more beneficial than understating it.

Given these values, the transverse impedance as a function of frequency and phase advance is determined.

In the infinitely periodic structure without damping, the beam sees the transverse impedance values along the speed of light line $\phi = \omega l/c$, whose real part is nonzero only at discrete frequencies. In the damped case, the resonances spread out such that there is interaction with the beam for a continuous range of synchronous phases and frequencies. In this case, the consistent description is no more a Brillouin diagram giving the eigenfrequency as a function of the phase advance, but a two dimensional impedance function depending on frequency and phase (figure 3).

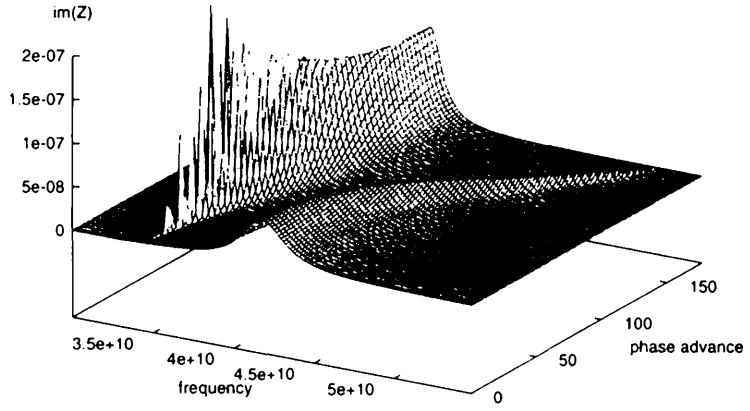

Figure 3: Imaginary part of the transverse impedance versus frequency and phase advance.

The equations for the damped detuned structure are set up in the usual manner, calculating several sample cells and interpolating the values in order to obtain the parameters for all. With v_i and $\hat{v}_i$ as normalized TE and TM circuit voltages, i_i as the driving beam current and $k_{x,i} = \sqrt{k_i \hat{k}_i}$ as the TM/TE coupling, one obtains the following equation system:

$$\begin{aligned}
\frac{k_{i-1/2}}{2} v_{i-1} + (x_i - \lambda) v_i + \frac{k_{i+1/2}}{2} v_{i+1} - \frac{k_{x,i-1/2}}{2} \hat{v}_{i-1} + \frac{k_{x,i+1/2}}{2} \hat{v}_{i+1} &= 0 \\
-\frac{\hat{k}_{i-1/2}}{2} \hat{v}_{i-1} + (\hat{x}_i - \lambda) \hat{v}_i - \frac{\hat{k}_{i+1/2}}{2} \hat{v}_{i+1} + \frac{k_{x,i-1/2}}{2} v_{i-1} - \frac{k_{x,i+1/2}}{2} v_{i+1} &= \sqrt{A_i} i_i
\end{aligned}$$

Due to nonlinearities, solving the system via eigenvalues is impractical, so the approach used in [3] is followed by solving directly for the circuit voltages as a function of frequency and beam current. With the right ordering of the unknowns, the equations form a narrowly banded matrix, for which efficient solution algorithms exist.

Skeleton design

Using this modeling approach a skeleton design has been made. The label skeleton is used, because things such as the electrical parameters of the load material in the range of 30-60 GHz and the precise load geometry are not known for the time being. The idea is to get basic performance data in connection with a 'minimum performance' waveguide load.

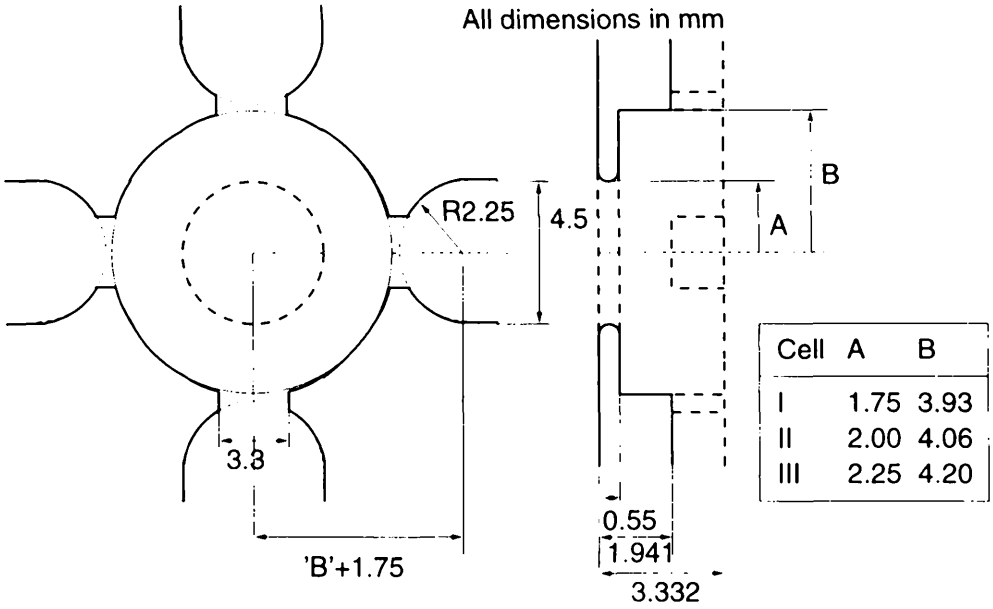

Figure 4: Cell geometry used for the skeleton design.

In this step, more realistic cell geometries shown in figure 4 have been used. Apart from differing dimensions, the basic change from the generic cells used before is that the waveguide height no longer equals the cell length. In order to improve the mechanical rigidity, it has been reduced and is placed asymmetrically with respect to the cell.

This has the following implications. The cell geometry is no longer symmetrical with respect to the longitudinal axis. Where in the generic case the coupling between the TE cavity mode and the TE_{10} waveguide mode was exactly zero due to symmetry, this holds only in the approximative sense for a non symmetric cell. With a coupling strength equivalent to a damped Q of 16 for a pure TM mode, there is now a damping corresponding to a Q between 80 and 130 for the TE_{π} resonance. This has been taken into account in the following results by assuming a flat Q of 200 in the TE circuit equations (The Q factors mentioned above assume ideal non reflecting waveguide loads!). The equivalent circuit parameters are given in table 3.

For the detuning the distribution shown in figure 5 was used. The corresponding dn/df density function can be labelled as a smoothed quasi constant gradient distribution following the generic density function:

$$\frac{dn}{df} = \sqrt{1 - x^2}; |x| < 0.996$$

That way, the initial roll off is improved from the $\sin x/x$ behavior, one would expect in a pure constant gradient type density.

For the waveguide load, a mechanically simple design has to be used, because structural dimensions become very tiny at 30 GHz. As absorbing material a silicon

cell	I	II	III
a/mm	1.75	2.0	2.25
b/mm	3.93	4.06	4.20
TE_0/GHz	38.68	35.10	32.02
TE_π/GHz	53.64	53.44	52.64
TM_0/GHz	43.09	41.92	40.82
TM_π/GHz	39.38	37.86	36.80
$\alpha \cdot 10^4$	1.51	1.69	1.65
Δ/mm	1.10	0.85	0.64
$\tilde{\alpha} \cdot 10^4$	1.73	1.65	1.55
$\tilde{\Delta}$/mm	1.13	0.95	0.75
A	214.95	152.41	109.88

Table 3: Equivalent circuit parameters for first, middle and last cell. $\tilde{\alpha}$ and $\tilde{\Delta}$ denote the values obtained by the TM_0 fit. For the precise definition of Δ see page 4.

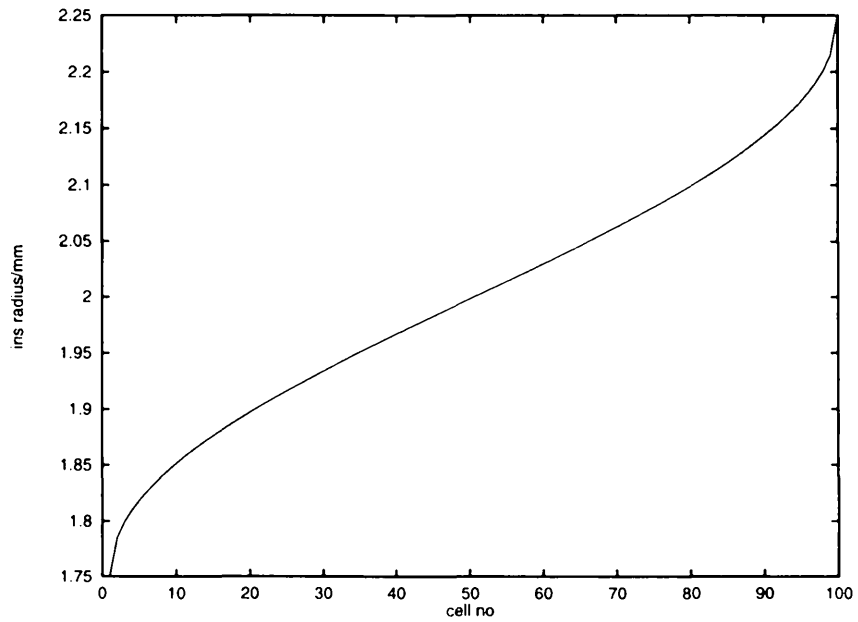

Figure 5: Iris radius versus cell number

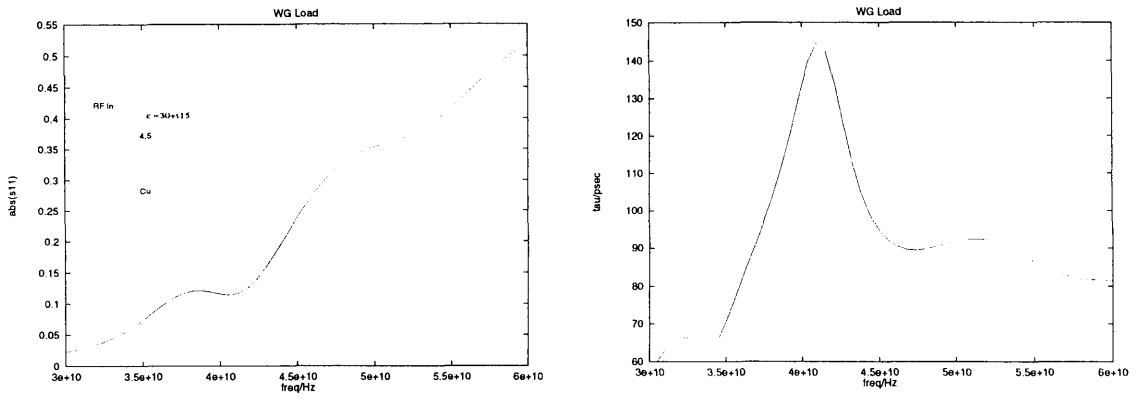

Figure 6: Amplitude and group delay of the waveguide load used.

carbide variant used in the KEK C-band project was used, whose electric constants in the range of 3-20 GHz are known as $\epsilon = 30 \ldots 40$ and $\tan\delta = 0.5 \ldots 0.6$ [4]. The behavior above 30 GHz is not known for the time being. For the simulations a constant dielectric constant of $\epsilon = 30$ and a loss angle of $\tan\delta = 0.5$ for all frequencies was assumed.

Apart from the vacuum properties, one of the advantages of SiC lies in the fact, that it behaves more like a bad conducting metal than a typical dielectric. Replacing the side wall of the waveguide with SiC gives already a good absorption behavior near the cut-off frequency. The design uses a waveguide length of 10 mm, the width of the guide slowly tapers down from 4.5 mm to 4 mm in order to improve the absorption at higher frequencies. Graphs of the reflection coefficient as well as the group delay is shown in figure 6.

With an ideal load with zero reflection, the choice of the length of the connecting waveguide between cell and load would be dictated only by mechanical considerations as well as the fact, that the fundamental mode should not leak into the load material. With non zero reflections, this length causes a transformation of the input impedance of the load depending on the frequency, leading to an oscillation of the wake impedance versus frequency. One approach is to choose a length where this oscillation actually widens the peak of the damped cavity resonance, obtaining a faster roll-off of the time domain wake. Additionally one can vary the waveguide length from cell to cell. Seen in the time domain, this means, that wake fields, reflected by the different loads, return into the cells with a slightly different group delay, lowering the integral wake. For the design only two different lengths of 6.5, resp. 7.5 mm (measured as described before) were chosen, alternating from cell to cell. The resulting wake function is shown in figure 7.

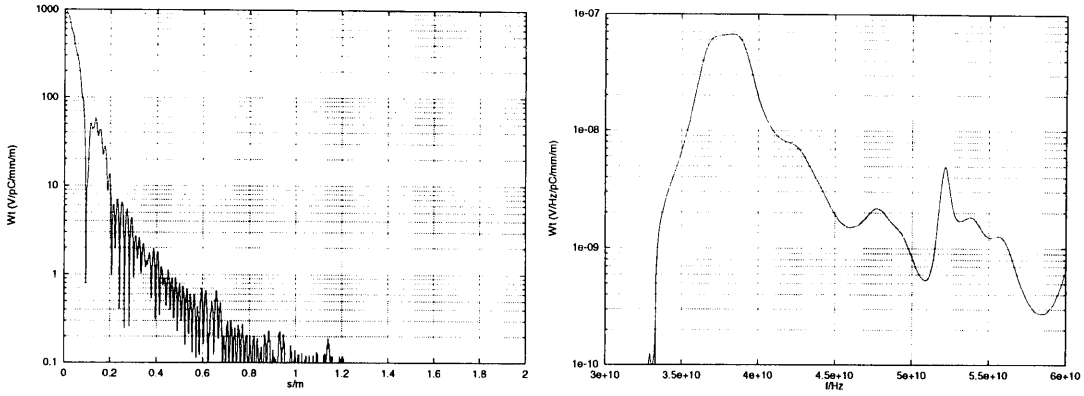

Figure 7: Time domain wake and impedance of the skeleton design.

Outlook

One of the questions still open at the moment concern the final load design. As yet, there are no reliable figures on the behavior of load materials in the range 30-60 GHz. Furthermore the final waveguide load will contain pumping ports and maybe other mechanical changes which will influence the load performance. But the requirements for the performance are not too high, and can in principle also be compensated by a more sophisticated detuning of the cells and/or using 4 or more different waveguide lengths between cell and load.

Another question concerns the equivalent circuit model itself. For the lower two dipole bands the similarity between the equivalent circuit results and MAFIA results is quite good. Possible inaccuracies stem from the fact, that the circuits have been fitted using MAFIA results, which unavoidably contain numerical errors. Since these results can also be obtained to a large part via a measurement of sample cells, a correction is quite straight forward. The big interest anyway lies in a good accuracy for the detuning range, that is in the change of dipole frequencies from cell to cell, and not in a high absolute accuracy of the calculations.

The circuit model itself only describes contributions of the first two bands. This leaves the question of the magnitude of the very high frequency dipole wake. Trying to neglect a possible damping and to do a kind of uncoupled detuned analysis has been shown to be relatively impractical since, due to the waveguides, there is a high number of dipole bands, being hybrids of waveguide and cavity resonances.

The last question is a possible asymmetry in the loads causing the reflected power from the loads to come back with a different timing and magnitude. This would enable monopole wakes, where the sign of the wave is equal in all waveguides, to convert into dipole wakes, where the signs are opposite. Alternatively, one can say that the electrical field center of the higher order modes has been shifted from the geometrical center of the cell.

Given the fact that this is a random error occurring in every cell, there is a partial cancellation inside the structure leading to an r.m.s. error of the total structure, which is

smaller by a factor $\sqrt{N}$ (N the number of cells in the structure) than that of a single cell. Allowing for a shift of the center equal to the alignment tolerance of 10 μm, the center in a single cell can be off by 100 μm (assuming 100 cells). Concerning mechanical asymmetries, there should not be a problem in staying below this threshold.

With regards to the electrical properties of the load material, things might be different. Apart from the fact that the load determines the magnitude of the reflection, it also has a quite significant influence on the group delay, that is the time, after which the reflected wave returns to the cavity. For the waveguide load used, the variation of the group delay of the order of 60 picoseconds is equivalent to a variation of the electrical length of 9 mm. Therefore variations in the dielectric or absorption parameters might have a significant effect, which should be further examined.

References

[1] K. Bane, R. Gluckstern, *The transverse wakefield of a detuned X-band accelerator structure*, Particle Accelerators, Vol. 42, pp. 213 (1993).

[2] N.M. Kroll, D.U.L. Yu, *Computer determination of the external Q and resonant frequency of waveguide loaded cavities*, SLAC-PUB-5171 (1990).

[3] R.M. Jones, K. Ko, N.M. Kroll, R.H. Miller, *A spectral function method applied to the calculation of the wake function of the NLCTA*, proc. LINAC 96, Geneva Switzerland (1996).

[4] H. Matsumoto, private communication.